A novel approach to blastocyst quality assessment using deep learning TLI image analysis

Rong-Yu Wu
Department of Electrical Engineering
National Taiwan Ocean University
Keelung 20224, Taiwan
abner90635@gmail.com

Huai-Wen Chang
Department of Electrical Engineering
National Taiwan Ocean University
Keelung 20224, Taiwan
huaiiwenn@gmail.com

Ming-Jer Chen
Division of Infertility
LeeWomen's Hospital
Taichung 40705, Taiwan
mingjerchen@gmail.com

Yu-Chiao Yi
Division of Reproductive
Endocrinology and Infertility
Veterans General Hospital (VGHTC)
Taichung 40705, Taiwan
yuchiaoyi@gmail.com

Shih-Kai Lee
Department of Electrical Engineering
National Taiwan Ocean University
Keelung 20224, Taiwan
wax78216@gmail.com

Ren-Jie Huang
Department of Electrical Engineering
National Taiwan Ocean University
Keelung 20224, Taiwan
jajs8869@gmail.com

Jung-Hua Wang*
Department of Electrical Engineering
National Taiwan Ocean University
Keelung 20224, Taiwan
jhwang@email.ntou.edu.tw

Abstract—**Infertility, defined as the inability to conceive after 12 months of regular and unprotected intercourse, has been rising due to factors like environmental hormones and late marriages, increasing the demand for assisted reproductive technology (ART). Machine learning, particularly deep learning (DL) models trained with time-lapse incubator (TLI) video images, can improve the success rates of infertility treatments by providing valuable morphokinetic parameters for embryo assessment. This paper introduces two novel DL algorithms for TLI image analysis: Algorithm_1 is based on instance segmentation to train two different YOLOv5 models, doing so helps enhance the efficacy of segmenting cells of trophectoderm (TE), achieving 81.1% recall and 79.9% precision. Results of YOLOv5 are also used to count TE cells and quantify the area ratio of ICM and TE vs. blastocyst. Based on cell texture changes, we apply GLCM analysis of ICM images to distinguish Gardner grades A and B. Algorithm_2 uses confidence level to determine the time point (CDTP) with three separate ResNet50-based models for identifying tSB, tB, and tEB, respectively. With 94% accuracy, timestamps of tSB, tB, and tEB are identified and compared with the machine-marked stamps by the original maker. Our method gives an average time difference of 1.99 hours from the ground truth, much less than the 3.87 hours by Vitrolife™. The proposed two algorithms can effectively enhance the prediction and assessment of embryonic growth stages.**

Keywords—time-lapse incubator, deep learning, classifier, Texture analysis, instance segmentation
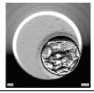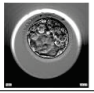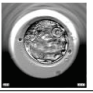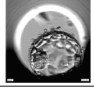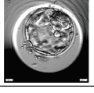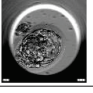
I. INTRODUCTION AND RELATED WORK

In studies of blastocyst characteristics, the Gardner grading system [1] serves as the primary method of assessment, evaluating embryos based on three parameters: blastocyst development stage, inner cell mass (ICM) quality, and trophectoderm (TE) quality, as illustrated in TABLE I. The Gardner grading system is inherently subjective, as individual embryologists at medical institutions responsible for grading are bound to have personal preferences. In addition, embryologists also need to spend a lot of time observing embryo images to obtain grading, making obtaining consistent and objective grading results difficult. However, with the advancement of technology, including the introduction of time-lapse incubators (TLI) and the development of powerful deep learning (DL) technology, a more objective assessment of blastocyst quality can be achieved. In light of this, this paper proposes two novel algorithms. The first (**Algorithm_1**) involves analyzing embryo images of embryo quality, and the second (**Algorithm_2**) focuses on the timestamp prediction of embryonic growth stages.

A. Use of Image Segmentation and Texture Analysis

Infertility research has gradually adopted TLI Images as input data, primarily for morphometric analysis. This involves extracting embryonic dynamics parameters from TLI Images, which can assist in making decisions in embryo selection, embryo implantation, and pregnancy prediction. Additionally, vast research works have accumulated a huge amount of data suitable for training deep neural networks[2]. Deep learning excels at processing large data sets, allowing the model to understand or extract information contained in the data. For image analysis at the blastocyst stage, the traditional Gardner grading system relies on manual observation and is easily affected by subjective bias. Considering the variability of subjective judgments, a deep learning model is an ideal alternative in enhancing the objectivity of blastocyst grading.

According to the study in [3], after applying U-Net for semantic segmentation on TLI Images, the average expansion rate of euploid blastocysts that successfully survived was significantly higher than those not survive. Furthermore, the expansion rate of euploid blastocysts was significantly correlated with live birth rates, indicating that changes in expansion rate can serve as a basis for predicting live birth rates. Results of [4] shows that, after using convolutional neural networks (CNN) and recurrent neural networks (RNN) to train models for grading the inner cell mass (ICM) and trophectoderm (TE) into three different grades A, B, and C, the resulting morphological grades of ICM and TE were used to obtain 0.66 of Area Under the Curve (AUC), which is slightly higher than the 0.64 achieved by embryologists. Although such prediction performance of machine learning was slightly better than that of embryologists, statistical analysis showed no significant difference between the two (p=0.536). This suggests that machine learning can potentially

TABLE I Gardner grading system

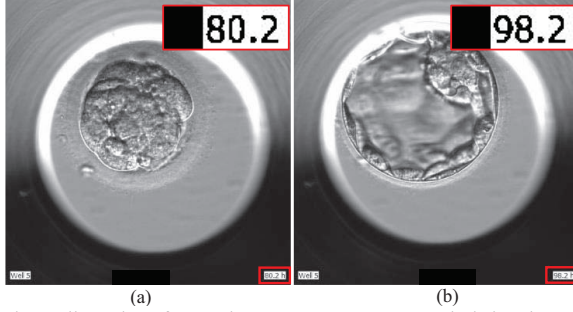| ICM quality	A	B	C
Schematic			
	Tightly packed, many cells	Loosely grouped, several cells	Very few cells
TE quality	A	B	C
Schematic			
	Many cells forming a tightly knit epithelium	Few cells	Very few cells forming a loose epithelium

Fig. 1 Illustration of OCR timestamp capture process, depicting the same process for both (a) and (b).

improve outcomes in infertility treatment, but further research is needed to validate its benefits.

The study of [5] evaluated the texture of mouse embryos through fluorescence measurement. The results indicated that Gray Level Co-occurrence Matrices (GLCM) [6] can effectively extract information on the fluorescence emission microstructure in embryos. Further quantization work of [5] demonstrated that using GLCM metrics to analyze fluorescent textures can identify metabolic changes during embryonic development. In 2018, [7] used shape and texture features to predict the birth weight and FGR of healthy fetuses and FGR (fetal growth restricted) fetuses, and the accuracy of identifying FGR pregnancy reached 86%. GLCM is highly effective in extracting information from medical images. Its strengths are particularly notable in anatomical structure segmentation, lesion detection, and distinguishing between pathological and healthy tissues, underscoring its potential applications in reproductive medicine. This paper aims to utilize YOLOv5 [8] to perform instance segmentation for extracting image features of blastocysts, trophectoderm (TE), and inner cell mass (ICM), and for performing texture analysis based on these features.

Research [9] shows that the higher the blastocyst diameter to ICM diameter ratio, the higher the pregnancy success rate. Therefore, the area and maximum width of the blastocyst can be used as indicators to evaluate the pregnancy rate. Reference [10] shows that each one μm increase in blastocyst width and each one μm² increase in blastocyst area raises the probability of pregnancy by 2.6% and 0.008%, respectively. This indicates a significant correlation between blastocyst size and pregnancy outcomes. According to [11], the higher the Gardner grade of TE, the higher the pregnancy rate, but it is not significantly related to the live birth rate. To extract blastocyst information from TLI images, our method uses YOLOv5 to extract masks from the images of the blastocyst, ICM, and TE cells and performs quantification the area ratio of ICM vs. the entire blastocyst, thereby yielding more objective results.

B. Morphokinetic Analysis

In morphokinetic analysis, many studies on blastocyst developmental stages use *time of starting blastulation* (tSB), *time of full blastocyst* (tB), and *time of expanding blastocyst* (tEB) as the main observation time points. According to a study on intracytoplasmic sperm injection (ICSI) treatment [12], the critical time parameter tSB can be categorized into two kinds of interval: long (96 to 114 hours) and short (78 to 95.9 hours). Embryos in the short interval have a significantly higher implantation than those in the long interval. Studies of [13] indicate that for each additional year of maternal age, the

time for the embryo to reach tB increases by 0.78 hours, and the interval from the time of morula (tM) to tSB increases by 0.92 hours. Research [14] found that the average interval from pronuclear decay (tPNf) to tSB in newborns with congenital anomalies was significantly longer than in healthy newborns. Furthermore, the mean tPNf to tSB interval was significantly longer in neonates of gestational diabetic mothers than in neonates of normoglycemic mothers. According to [15], live birth outcomes can be predicted based on the hours post insemination (HPI) on day 5, blastocyst morphology, and maternal age.

The aforementioned studies all claimed the importance of morphokinetic parameters in ICSI and IVF treatments because early infertility research heavily relies on manually annotating morphokinetic parameters, a process that is both time-consuming and labor-intensive. In view of this, this article employs machine learning to analyze TLI images and extract morphokinetic parameters for distinguishing blastocyst developmental stages, thereby saving embryologists' time.

II. METHODOLOGY

We develop two algorithms to extract blastocyst morphokinetic parameters from TLI Images. In **Algorithm_1**, TLI images are processed by two deep learning models, *model_yolo* and *model_yolo_TE*. The *model_yolo* is used to obtain segmentation results for the blastocyst, inner cell mass (ICM), and trophectoderm (TE) cells, while *model_yolo_TE*, through an *Image_Crop* step to enhance recall and precision for TE cells, is specifically used to obtain segmentation results for TE cells. These prediction results can be used to quantify the area ratio of ICM and TE relative to the blastocyst and to perform texture analysis on the segmented ICM images to distinguish between Gardner grades A and B. **Algorithm_2** uses multiple ResNet50 [16] models to distinguish growth categories in the blastocyst stage. Using the *CDTP* step, the classification is determined based on confidence levels to identify the initial images of tSB, tB, and tEB, followed by applying Optical Character Recognition (OCR) [17] to obtain the starting timestamps for each category.

A. Data Collection

Our data comes from non-public, de-identified TLI Images provided by the Department of Obstetrics and Gynecology of Taichung Veterans General Hospital (VGHTC) from 2021 to 2023. The data set is annotated by the hospital's internal professional medical team. The YOLOv5 model used a dataset consisting of 453 training images, 151 verification images, and 65 test images; the Resnet50 model used a dataset consisting of 6,406 training images, 1,511 verification images, and 743 test images. All images have a resolution of 500x500 pixels.

According to Article 12, paragraph 2 of the Taiwan Human Research Act, "*Research protocol shall obtain the consent of participating research subjects as approved by the IRB. But the research protocol within the scope of exemption categories for consent requirements, as announced by the competent authority, shall not apply*." The Taiwan Centers for Disease Control and Prevention issued an official document (code:1010265083). The method of obtaining the research data complies with the second and third items of the above announcement, so waiver of informed consent.
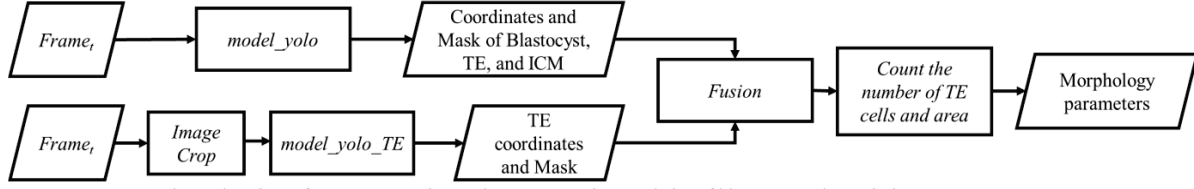
Fig. 2 Flowchart of **Algorithm_1** that analyzes texture characteristics of blastocyst and morphology parameters
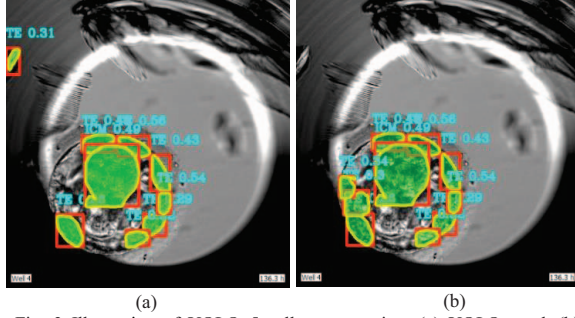

(a)   (b)

Fig. 3 Illustration of YOLOv5 cell segmentation: (a) YOLO result;(b) *Fusion* result.

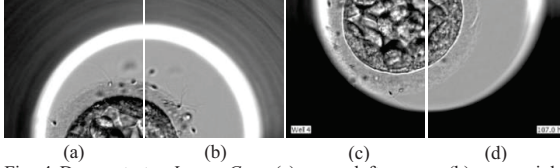(a)   (b)   (c)   (d)

Fig. 4 Demonstrates *Image Crop* (a) upper left corner, (b) upper right corner, (c) lower left corner, (d) lower right corner.

B. Improved Instance Segmentation Results Via Fusion

In Algorithm_1, we utilize YOLOv5 to extract instance segmentation results of the blastocyst, ICM, and TE cells. These segmentation results can be used to calculate parameters such as area, number, and texture features (Fig. 2). Algorithm_1 comprises two YOLO models: model_yolo, trained on blastocyst, ICM, and TE cells, and model_yolo_TE, trained exclusively on TE cells. Both use TLI images as input.

The *model_yolo* segments the TLI Images into three categories: blastocyst, ICM, and TE cells, and then extracts the coordinates and masks for each category. Since *model_yolo* performs poorly on precision and recall of TE cells, we trained a model focused on TE prediction, named *model_yolo_TE*. To enable *model_yolo_TE* to clearly identify TE cells in images, we performed an *Image Crop* preprocessing step before training. This step involved cropping the TLI Images (*Frame_t*) into four equal-sized square images along half its side length (Fig. 4). To address the issue of the embryo potentially not appearing in the cropped image due to movement in the petri dish, the *Image Crop* step included a check process that excluded images without cell labels from the training set. This approach enhanced the model's ability to focus on local features, reduced interference from other labels, and ultimately improved the segmentation performance of *model_yolo_TE*, producing accurate coordinates and masks of TE cells. Finally, we applied a *Fusion* step to integrate the segmentation results of *model_yolo* and *model_yolo_TE* to enhance the segmentation quality of TE cells. This step paired the segmentation results from both models based on their Intersection over Union (IoU) of masks and the distance between coordinates. If *model_yolo*

did not effectively segment certain TE cells but *model_yolo_TE* did, the TE cell segmentation results from *model_yolo_TE* were merged. To address potential false positives in the results of *model_yolo_TE*, we used the blastocyst mask from *model_yolo* to exclude any TE cells located outside the blastocyst region. Fig. 3(a) illustrates the segmentation result of *model_yolo*, while Fig. 3(b) shows the result after applying the *Fusion* step. This approach effectively mitigates false positives in TE cell segmentation and integrates the results of coordinates and masks, thereby providing a robust foundation for subsequent quantitative analyses of cell number and area.

C. Texture Analysis for Grading ICM

The well-known GLCM generates six critical features for texture analysis: Angular Second Moment (ASM), Homogeneity, Entropy, Contrast, Dissimilarity, and Correlation. These six features are a subset of the critical texture features obtained from the GLCM [7]. ASM reflects the overall homogeneity of the image, with higher values indicating a more uniform texture. Homogeneity measures the similarity of grayscale values among neighboring pixels, with higher values reflecting greater local texture uniformity. Entropy quantifies the randomness of texture changes within the image, with higher values denoting more pronounced randomness. Contrast represents the magnitude of grayscale level changes, with higher values indicating more prominent texture variations. Dissimilarity quantifies the grayscale differences between adjacent pixels, with higher values indicating more noticeable texture changes. Correlation assesses the linear relationship between pixels, with higher values indicating stronger linear relationships. Collectively, these features offer a detailed characterization of image texture.

This section uses GLCM to analyze the texture on the ICM mask (Fig. 5) extracted by **Algorithm_1**, aiming to identify texture differences between grade A and grade B ICM by analyzing the key texture feature values generated through GLCM. VGHTC employed the Gardner grading system to classify ICM quality into Due to the much smaller sample size in grade C, this study focuses only on grades A and B for GLCM calculations. Because each embryo has a different number of ICM mask images at the blastocyst stage, we designed a method to normalize the ICM feature values. The details of the method are as follows: Assume that L represents
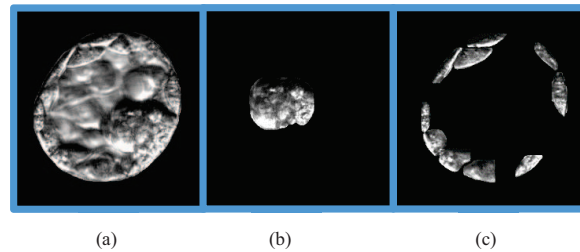

(a)   (b)   (c)

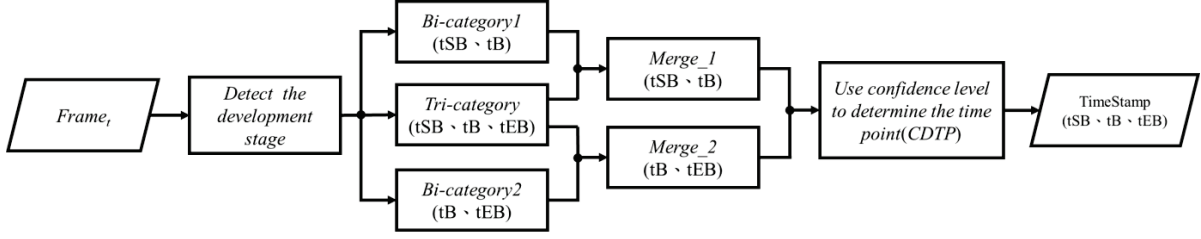Fig. 5 YOLOv5 extract mask(a)blastocyst mask;(b) ICM mask; (c)TE mask

Fig. 6 Flowchart of **Algorithm_2** for identifying the timestamp of the development stages of blastocyst.

a list containing GLCM values under different features. N is the number of L, T is the target value after the normalization of the features, and Q represents the number of blastocysts. (1) F refers to six indicator parameters. (2) L is a numerical array corresponding to specific F parameters. (3) g is the quotient obtained by dividing N by T. (4) r is the remainder obtained by dividing N by T. (5) $X_J^{F_i}$ represents the values after normalization for the Jth embryo, where J ranges from 1 to Q. (6) If N cannot be evenly divided by T in the normalization process, one more value is added in the averaging process of the first r terms. For terms beyond the first r, only g values are averaged. (7) Y records k feature values y_k, where k ranges from 1 to T. Each y_k is obtained by averaging the corresponding feature values x_{jk} across Q blastocysts.

$$F = \left\{ \begin{array}{c} ASM, Entropy, Contrast, \\ Dissimilarity, Homogeneity, Correlation \end{array} \right\} \quad (1)$$

$$L = \{Value_1^F, Value_2^F, \cdots, Value_N^F\} \quad (2)$$

$$g = div(\frac{N}{T}) \quad (3)$$

$$r = mod(\frac{N}{T}) \quad (4)$$

$$X_J^{F_i} = \{x_{j1}, x_{j2}, \cdots, x_{jk}\} \ ,$$
$$J \in \{1, 2, \cdots, Q\} \quad (5)$$

$$x_{jk} =$$

$$\begin{cases} \frac{1}{g+1} \sum_{i=1}^{g+1} Value_{(k-1)(g+1)+i}^F & , k \in \{1, 2, \cdots, r\} \\ \frac{1}{g} \sum_{i=1}^{g} Value_{(k-1)(g+1)+i}^F & , k \in \{r+1, r+2, \cdots, T\} \end{cases} \quad (6)$$

$$Y^{F_i} = \{y_1, y_2, \cdots, y_k\}; y_k = \frac{1}{Q} \sum_{j=1}^{Q} x_{jk} \ , \quad (7)$$
$$k \in \{1, 2, \cdots, T\}$$

This method normalizes the varying number of images at the blastocyst stage for each embryo, enabling robust comparison of texture differences between grade A and grade B ICM and providing valuable data for assessing ICM grading.

D. Deep Learning Image Classifier

Algorithm_2 (Fig. 6) utilizes ResNet50 to capture the time of starting blastulation (tSB), the time of full blastocyst (tB), and the time of expanding blastocyst (tEB). Given that TLI images represent temporal data, we first trained a three-category model named *Detect the Development Stage (DDS)* to classify TLI Images into embryo, blastocyst, and End stages (Fig. 7). To further classify blastocyst images into tSB, tB, and tEB, we developed three additional ResNet50 models: *Tri-category*, *Bi-category1*, and *Bi-category2*. While the *Tri-*

category model classifies all three sub-categories simultaneously, due to its suboptimal performance in classifying tSB, We introduced two binary models, *Bi-category1* and *Bi-category2*, to simplify the complexity of the task of the *Tri-category* classifier. After the *DDS* model identifies the blastocyst stage images, these images are simultaneously input into *Bi-category1*, *Tri-category*, and *Bi-category2* for further classification. The results from *Bi-category1* and *Tri-category* are merged into *Merge_1*, and the results from *Bi-category2* and *Tri-category* are merged into *Merge_2*. We *use confidence levels to determine the time point (CDTP)* step to compare outputs from *Merge_1* and *Merge_2* and select the classification with the higher confidence value to identify the image as tSB, tB, or tEB. Finally, we identify the earliest images for each category and extract their timestamps using OCR to obtain the starting times of tSB, tB, and tEB.
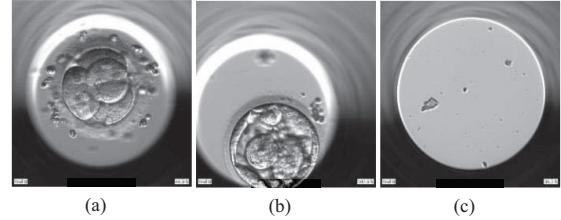

Fig. 7 Illustrates the differentiation of blastocyst stages using the Stage Distinction method. (a) embryo stage, (b) blastocyst stage, and (c) the blastocyst is removed named End

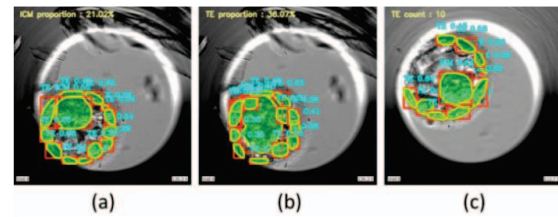Fig. 8 YOLOv5 confusion matrix(a)YOLO result;(b) *Fusion* result

Fig. 9 Diagram of cell characteristics(a) area ratio of ICM is 21.02%;(b) area ratio of TE is 36.07%; (c) here the number of TE is 10.
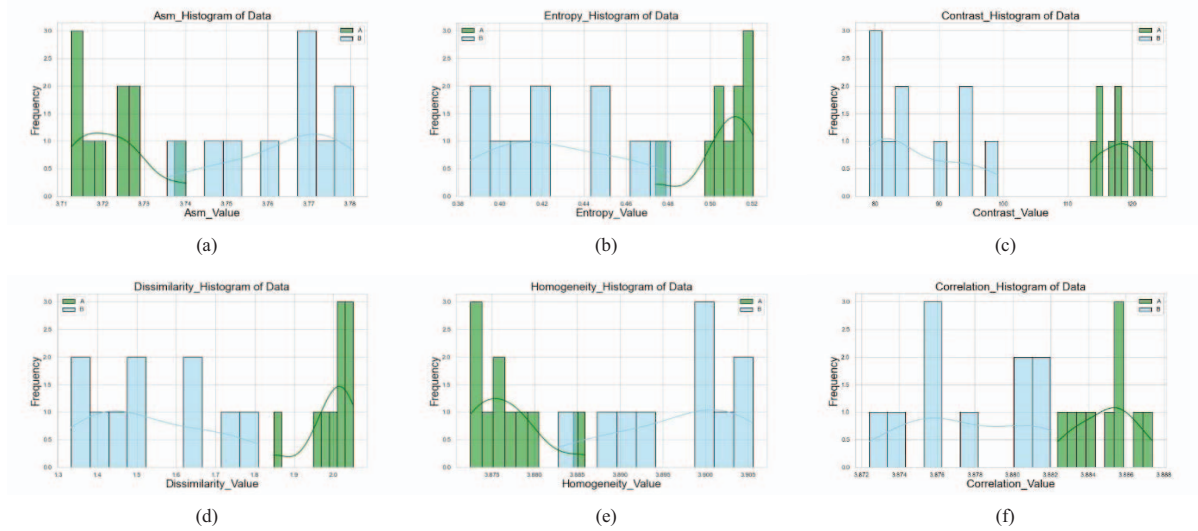
Fig. 10 Displays the GLCM result histograms for various texture analysis metrics (a)ASM; (b)Entropy; (c)Contrast; (d)Dissimilarity; (e)Homogeneity; (f)Correlation

III. RESULT

A. Equipment

Hardware: CPU i9-9900 with on NVIDIA GPU/RTX-2080 and RAM/32G. Software: Windows10, Python 3.8, Cuda 11.1, cuDNN 8.0.5.

B. Time Lapse Image Analysis

The method was validated using 65 blastocyst images. Fig. 8(a) presents the confusion matrix of TE cells for segmentation by *model_yolo*, which achieved a recall of 77.2% and a precision of 61.1%. However, the real breakthrough is depicted in Fig. 8(b), which demonstrates a remarkable performance improvement in the segmentation of TE cells after *Fusion*, with recall increasing to 81.1% and precision to 79.0%. This significant progress underscores the effectiveness of our method. Fig. 9(a) illustrates the area ratio of ICM to the entire blastocyst, Fig. 9(b) illustrates the area ratio of TE cells to the entire blastocyst, and Fig. 9(c) shows the number of TE cells. Fig. 10 presents distinct GLCM texture analysis results for ICM grades A and B. In Fig. 10(a), ASM results indicate that grade B textures are more uniform and less variable than grade A. Fig. 10(b) shows that grade A textures are more complex and variable in Entropy. Fig. 10(c) and 10(d) reveal that grade A textures have more pronounced cell boundaries through higher Contrast and Dissimilarity. Fig. 10(e) highlights greater Homogeneity in grade B textures, while Fig. 10(f) demonstrates a stronger linear dependence correlation in grade A textures. This method revealed distinct histogram distributions for grades A ICM and B ICM, indicating significant differences in cell textures. These distribution disparities effectively distinguish between grades A ICM and B ICM.

C. Time Stamp Prediction

To demonstrate the effectiveness of *Bi-category1* and *Bi-category2*, we tested the *Tri-category* alone (without *CDTP*). The resulting confusion matrix is shown in Fig. 11(a), with an accuracy of 93%. In comparison, Fig. 11(b) displays the confusion matrix obtained from executing **Algorithm_2**, with the accuracy being improved to 94%. In this experiment, we used 743 manually classified images provided by VGHTC,

which served as the test set and the Ground Truth (GT). This test set encompasses data in three categories: tSB, tB, and tEB. We also compare the time points of six blastocysts using three sources: the manually annotated GT, data from Vitrolife™, and results from **Algorithm_2** developed in this study. The average time difference between the GT and Vitrolife™ data is 3.87 hours, while Algorithm_2 reduces the average difference to 1.99 hours.

TABLE II lists the time points of six blastocysts. **Algorithm_2**, designed with cost-effective deep learning, determines blastocyst growth stages, extracts timestamp from images and uses OCR for division time points. It provides more accurate time points than other methods (see TABLE II), which is crucial for analyzing implantation or pregnancy rates and enhances the credibility of quality assessments.

IV. CONCLUSION

Two deep learning-based algorithms have been presented to quantify blastocyst quality. First, blastocyst growth stages are classified via Resnet50 trained with TLI images. The design of *CDTP* involves the cooperation of one *Tri-category* model and two *Bi-category* models to improve the accuracy of identifying important time stamps of blastocyst development stages of tSB, tB, and tEB. Experimental results on 743 images show that, compared to the ground truth, our method can achieve a time difference of 1.99 hours, which is much less than the 3.87 hours reported by Vitrolife™. Secondly, YOLOv5 is utilized to generate plural masks for quantifying the number and area of TE, ICM, and blastocyst. The well-known GLCM texture analysis is conducted on the extracted ICM images to differentiate grade A from grade B by the distinct histogram distributions between the two grades. The beauty of the step of *Fusion* in Fig.2 is its provision of a compensating effect for *model_yolo* (i.e., the problem of poor prediction of TE), and the recall and the precision were improved from 61.1% to 81.1% and 77.2% to 79.9%, respectively.

TABLE II TimeStamp data of the six blastocysts

| Time-lapse image	Vitrolife™ TLI Report	Classifier Timestamp	Ground Truth
A	tSB:94.2 tB:102.9 tEB:110.5	tSB:96.5 tB:97.9 tEB:109.9	tSB:95.5 tB:97.9 tEB:109.2
B	tSB:80.5 tB:87.2 tEB:98.5	tSB:83.5 tB:84.5 tEB:98.2	tSB:82.5 tB:86.9 tEB:97.5
C	tSB:104.9 tB:123.8 tEB:130.9	tSB:107.6 tB:114.2 tEB:130.2	tSB:104.9 tB:118.2 tEB:130.5
D	tSB:112.7 tB:116.7 tEB:121.3	tSB:106.7 tB:109 tEB:119.3	tSB:108.3 tB:117.0 tEB:119.0
E	tSB:113.7 tB:132.0 tEB:140.7	tSB:124.5 tB:127.4 tEB:139.4	tSB:122.4 tB:128.4 tEB:139.0
F	tSB:96.4 tB:111.7 tEB:118.4	tSB:102.4 tB:104.7 tEB:117.4	tSB:100.4 tB:112.0 tEB:117.0
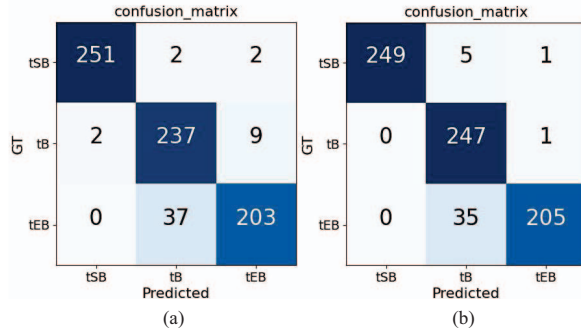
Fig. 11 Confusion matrix (a) using Tri-category model only result, accuracy=93%; (b) use both Bi-category and Tri-category as in Fig.6, accuracy=94%

In short, the major contribution of this study is that the two proposed approaches can be potentially used as practical tools to beneficially aid embryologists in their operation of embryo selection. Because TLI Images inherently contain abundant quantifiable spatiotemporal information which might affect infertility treatment, it can provide the potential for predicting implantation rates. In the future, it is expected that with more patients' blastocysts and annotated data, the method presented in this paper should be capable of analyzing TLI Images for extracting useful information other than the time stamps and morphokinetic parameters. In particular, when combined with physiological data, at least a higher implantation rate outcome, with intuition and interpretability, can be achieved with the presented algorithms.

REFERENCES

[1] Gardner. David. K, Schoolcraft. WB, "In-vitro culture of human blastocysts," *Towards reproductive certainty: infertility and genetics beyond 1999*, pp.378-388, 1999.

[2] Wang. JinLuan, et al., "Research progress of time-lapse imaging technology and embryonic development potential: A review," *Medicine*, Vol.102, No.38, pp.e35203.

[3] Huang. Thomas, et al., "Deep learning neural network analysis of human blastocyst expansion from time-lapse image files," *Reproductive Biomedicine Online*, Vol.42, No.6, pp.1075-1085, 2021

[4] Kragh. Mikkel. et al., "Automatic grading of human blastocysts from time-lapse imaging," *Computers in biology and medicine*, Vol.115, pp.103494, 2019.

[5] Tan. Tiffany. CY, et al., "Gray level Co-occurrence Matrices (GLCM) to assess microstructural and textural changes in pre-implantation embryos." *Molecular reproduction and development*, Vol.83, No.8, pp.701-713, 2016.

[6] Haralick. Robert. M, Shanmugam. Karthikeyan, and Dinstein. Its. Hak, "Textural features for image classification," *IEEE Transactions on systems, man, and cybernetics*, Vol.6, pp.610-621, 1973.

[7] Dahdouh. Sonia, "In vivo placental MRI shape and textural features predict fetal growth restriction and postnatal outcome," *Journal of Magnetic Resonance Imaging*, Vol.47 No.2, pp.449-458, 2018.

[8] Glenn. Jocher, et al., "ultralytics/yolov5: v3.1 - Bug Fixes and Performance," *Zenodo*, 2020.

[9] Almagor. Mriam, et al., "Ratio between inner cell mass diameter and blastocyst diameter is correlated with successful pregnancy outcomes of single blastocyst transfers," *Fertility and Sterility*, Vol.106, No.6, pp.1386-1391, 2016.

[10] Sciorio. Romualdo, et al., "Clinical pregnancy is significantly associated with the blastocyst width and area: a time-lapse study," *Journal of Assisted Reproduction and Genetics*, Vol.38, No.4, pp.847-855, 2021.

[11] Chen, Xiaojiao, et al., "Trophectoderm morphology predicts outcomes of pregnancy in vitrified-warmed single-blastocyst transfer cycle in a Chinese population," *Journal of assisted reproduction and genetics*, Vol.31, pp.1475-1481, 2014.

[12] Soukhov. Elena, et al., "Prediction of embryo implantation rate using a sole parameter of timing of starting blastulation," *Zygote*, Vol.30, No.4, pp. 501-508, 2022.

[13] Barrie. Amy, et al.,"An investigation into the effect of potential confounding patient and treatment parameters on human embryo morphokinetics," *Fertility and Sterility*, Vol.115, No.4, pp.1014-1022, 2021.

[14] Doron-Lalehzari. Alona, "Are morphokinetic parameters of embryo development associated with adverse perinatal outcomes following fresh blastocyst transfer?," *Reproductive BioMedicine Online*, Vol.42, No.1, pp.207-216, 2021.

[15] Liu. Yanhe, et al., "The effect of day 5 blastocyst assessment timing on live birth prediction and development of a prediction algorithm," *Reproductive BioMedicine Online*, Vol.44, No.4, pp.609-616, 2022.

[16] He. Kaiming, Zhang. Xiangyu, Ren. Shaoqing, and Sun. Jian, "Deep residual learning for image recognition," *In Proceedings of the IEEE conference on computer vision and pattern recognition* pp. 770-778, June. 2016. Las Vegas, NV, USA

[17] Islam. Noman, Islam. Zeeshan, and Noor. Nazia, "A survey on optical character recognition system," *arXiv preprint arXiv:1710.05703*, 2017.